Oligodendrocyte Lineage Transcription Factor 2 Inhibits the Motility of a Human Glial Tumor Cell Line by Activating RhoA

Kouichi Tabu,[1] Yusuke Ohba,[2] Tadaki Suzuki,[3] Yoshinori Makino,[3] Taichi Kimura,[1] Akiko Ohnishi,[4] Mieko Sakai,[1] Takuya Watanabe,[1] Shinya Tanaka,[1] and Hirofumi Sawa[3]

[1]Laboratory of Molecular and Cellular Pathology, [2]Laboratory of Pathophysiology and Signal Transduction, Hokkaido University School of Medicine; [3]Department of Molecular Pathobiology and 21st Century Center of Excellence Program for Zoonosis Control, Hokkaido University Research Center for Zoonosis Control, Sapporo, Japan; and [4]Department of Neurosurgery, National Cancer Center, Tokyo, Japan

Abstract

The basic helix-loop-helix transcription factor, oligodendrocyte lineage transcription factor 2 (OLIG2), is specifically expressed in the developing and mature central nervous system and plays an important role in oligodendrogenesis from neural progenitors. It is also expressed in various types of glial tumors, but rarely in glioblastoma. Although we previously showed that OLIG2 expression inhibits glioma cell growth, its role in tumorigenesis remains incompletely understood. Here, we investigated the effect of OLIG2 expression on the migration of the human glioblastoma cell line U12-1. In these cells, OLIG2 expression is controlled by the Tet-off system. Induction of OLIG2 expression inhibited both the migration and invasiveness of U12-1 cells. OLIG2 expression also increased the activity of the GTPase RhoA as well as inducing the cells to form stress fibers and focal adhesions. Experiments using short interfering RNA against $p27^{Kip1}$ revealed that up-regulation of the $p27^{Kip1}$ protein was not essential for RhoA activation, rather it contributed independently to the decreased motility of OLIG2-expressing U12-1 cells. Alternatively, semiquantitative reverse transcription-PCR analysis revealed that mRNA expression of RhoGAP8, which regulates cell migration, was decreased by OLIG2 expression. Furthermore, expression of C3 transferase, which inhibits Rho via ADP ribosylation, attenuated the OLIG2-induced inhibition of cell motility. Imaging by fluorescence resonance energy transfer revealed that in U12-1 cells lacking OLIG2, the active form of RhoA was localized to protrusions of the cell membrane. In contrast, in OLIG2-expressing cells, it lined almost the entire plasma membrane. Thus, OLIG2 suppresses the motile phenotype of glioblastoma cells by activating RhoA. (Mol Cancer Res 2007;5(10):1099–109)

Introduction

Gliomas are common primary tumors of the human central nervous system. Glioblastoma multiforme (also known as grade 4 glioma according to the WHO classification) is the most malignant type of glioma and is aggressive in terms of cell proliferation and migration. The invasiveness of glioblastoma multiforme, with its consequent diffuse infiltration into the surrounding brain tissue, is the major reason for the poor prognosis of affected individuals.

Oligodendrocyte lineage transcription factor 2 (OLIG2) is a member of the OLIG family of basic helix-loop-helix transcription factors. It plays a key role in the cell fate specification of oligodendrocytes and motor neurons in the dorsal spinal cord during development (1-4). It is also required for oligodendrogenesis from neural progenitor cells in the adult subventricular zone (5, 6). The abundance of OLIG2 mRNA and protein is increased in some human gliomas, and it has been suggested that OLIG2 is a potential diagnostic marker for oligodendrogliomas (7-9). Indeed, OLIG2 is readily detectable in tumors of the oligodendroglial lineage, which follow a relatively favorable clinical course. In contrast, OLIG2 expression is low or absent in glioblastomas (10-12). We have also shown that OLIG2 expression in glioblastomas is substantially lower than that in other types of glioma (13). To investigate whether the loss of OLIG2 expression contributes to the highly malignant behavior of gliomas, we previously established the U12-1 cell line, which is derived from the U251MG human glioblastoma cell line and which expresses OLIG2 under the control of the Tet-off system. We showed that inducing OLIG2 expression inhibits the proliferation and anchorage-independent growth of U12-1 cells (14). However, the role of OLIG2 in glioma cell motility remained unclear.

GTPases of the Rho family including Rho, Rac, and Cdc42 cycle between an active, GTP-bound state and an inactive, GDP-bound state (15). The active forms of these GTPases bind to various effector molecules that elicit downstream responses, including cell transformation (16-18), tumor cell invasion (19, 20), and metastasis (21, 22). These proteins also play important roles in the reorganization of the actin cytoskeleton during cell migration (23), as follows: activated Rho generates cell tension by inducing the formation of stress fibers and focal adhesions, which confer contractility on the cell body; activation of Rac results in the formation of membrane ruffles (lamellipodia), which are important in directed cellular movement, at the leading edge of the cell; and activated Cdc42 triggers the formation of membrane projections (filopodia), which are important determinants of cell polarity.

Here, we investigated the role of OLIG2 in the motility of U12-1 cells. We found that OLIG2 expression inhibited cell migration during wound closure *in vitro* as well as cell invasion through a Matrigel-coated filter. OLIG2 expression also increased RhoA activity as well as inducing the formation of stress fibers and focal adhesions. In addition, fluorescence resonance energy transfer (FRET) analysis revealed that in the absence of OLIG2, RhoA was specifically activated in membrane protrusions; in contrast, in cells expressing OLIG2,

activated RhoA was dispersed around almost the entire cell membrane. Together, our data suggest that OLIG2 suppresses the motility of glioma cells by regulating RhoA activity.

Results

OLIG2 Inhibits Human Glioblastoma Cell Migration and Invasion

We previously established a human glioblastoma cell line designated U12-1 in which OLIG2 expression is controlled by the Tet-off system. Thus, OLIG2 expression is induced in this cell line 24 h after removing doxycycline from the culture medium (14). To investigate the possible effect of OLIG2 on the migration of these cells, we compared cell motility in the absence or presence of OLIG2 expression by using an *in vitro* wound closure assay wherein the cell monolayer was given a linear scratch. After 24 h, Tet-on (OLIG2$^-$) cells covered most of the wounded area but the Tet-off (OLIG2$^+$) cells achieved only 38% of this degree of wound closure (Fig. 1A). To eliminate the possibility that this effect is due to OLIG2-induced modulation of cell proliferation, we repeated the assay in the presence of mitomycin C (10 μg/mL), which inhibits cell growth. We obtained essentially identical results (data not shown). Thus, OLIG2 inhibits the motility of U12-1 glioblastoma cells independently of any possible effect it may have on cell proliferation.
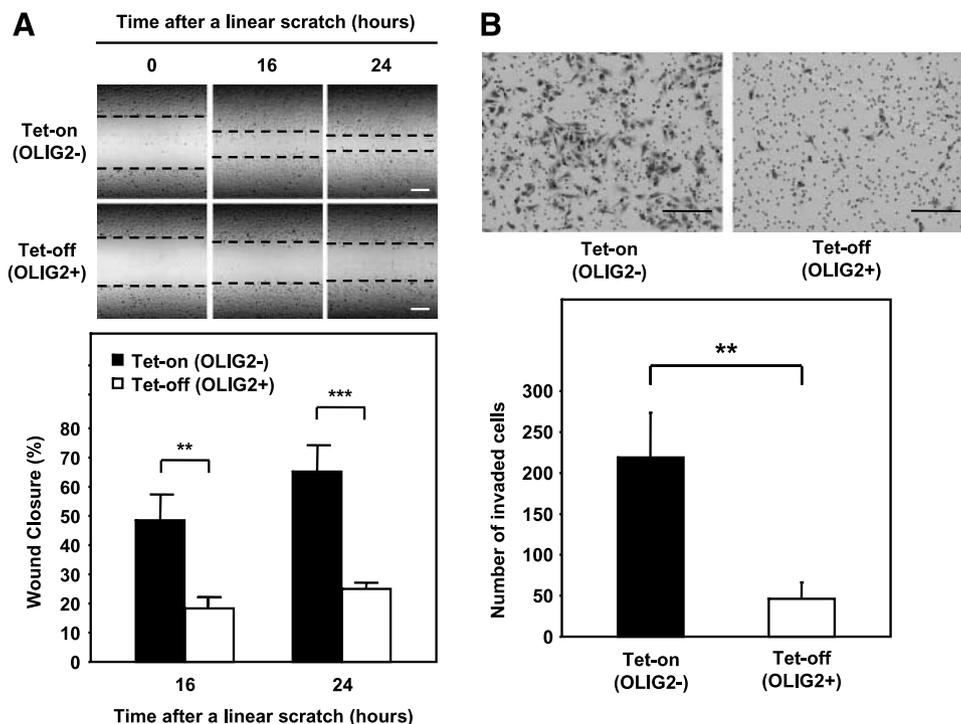
FIGURE 1. Inhibition of U12-1 cell migration and invasion by OLIG2. U12-1 cells were grown in Tet-on or Tet-off medium for 48 h and were then deprived of serum for 24 h. **A.** Cell migration. The U12-1 cells were wounded by introducing a linear scratch in the cell monolayer, followed by incubation in the corresponding complete medium for an additional 24 h. Top, representative micrographs of the wounded area (*dashed lines*) at the indicated times after wounding. Bars, 200 μm. Bottom, cell migration was evaluated by calculating the percentage of the width of the original scratch that was covered by migrating cells; columns, means of values from three independent experiments; bars, SD. **, $P < 0.01$; ***, $P < 0.001$ (Student's *t* test) for the indicated comparisons. **B.** Cell invasion. The U12-1 cells were harvested and allowed to invade a Matrigel-coated filter for 16 h. Top, representative micrographs of cells that had migrated to the lower surface of the filter. Scale bars, 200 μm. Bottom, cell invasion was quantified by counting the total number of cells on the lower surface of the filter in five random fields; columns, means of values from three independent experiments; bars, SD. **, $P < 0.01$ (Student's *t* test).
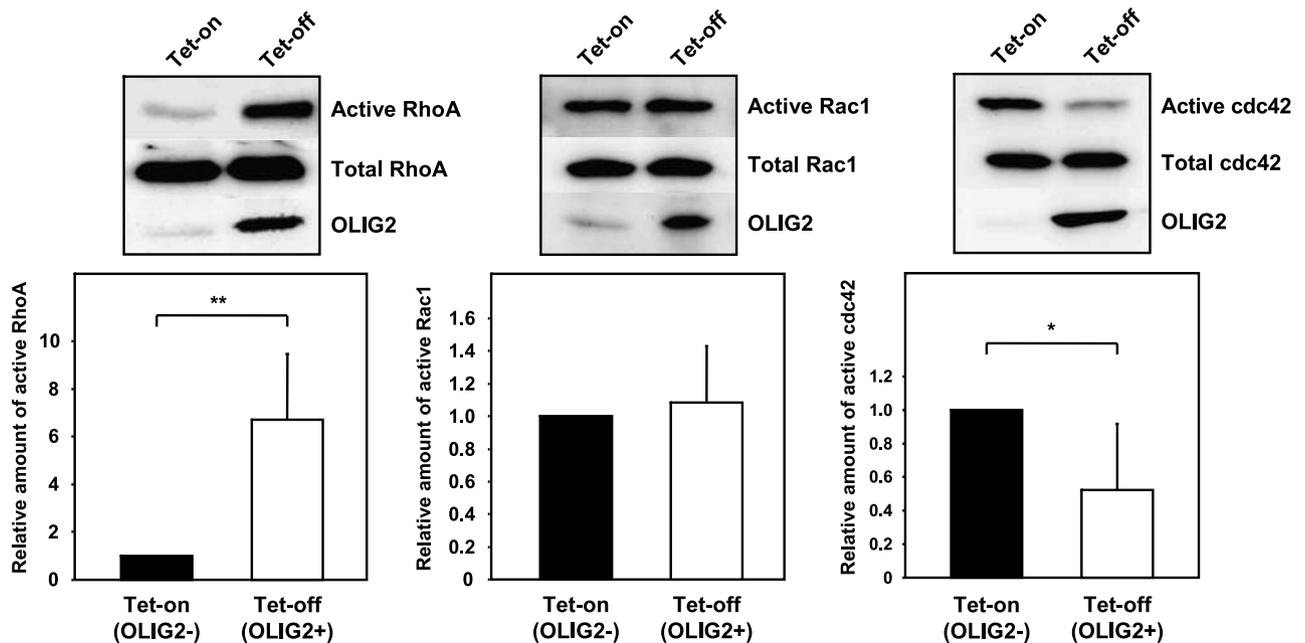
FIGURE 2. OLIG2 expression has different effects on the activity of Rho family GTPases. U12-1 cells were grown in Tet-on or Tet-off medium for 72 h, after which the active forms of Rho family GTPases were precipitated from cell lysates with either GST-Rhotekin-RBD (for RhoA) or GST-PAK2-CRIB (for Rac1 and Cdc42) immobilized on glutathione-Sepharose 4B beads. The precipitated proteins were then subjected to immunoblot analysis with antibodies specific for RhoA (*left*), Rac1 (*middle*), or Cdc42 (*right*). The cell lysates were also subjected directly to immunoblot analysis with the same antibodies as well as with antibodies specific for OLIG2. Top, the blots were subjected to densitometry to quantitate the active form of each GTPase (normalized by the corresponding total amount of the protein). Bottom, quantitative data from three independent experiments expressed relative to the corresponding value for Tet-on cells; columns, mean; bars, SD. *, $P < 0.05$; **, $P < 0.01$ (Student's *t* test).

We next examined the ability of OLIG2 to inhibit the invasion of U12-1 cells through a Matrigel-coated filter. Over a 16-h culture, significantly fewer OLIG2^{+} cells passed from the upper to the lower surface of the filter compared with OLIG2^{−} cells (Fig. 1B). Quantitative analysis revealed that OLIG2 reduced the invasiveness of U12-1 cells in this assay by 21% relative to control levels.

Matrix metalloproteinases (MMP) play an important role in the degradation of the extracellular matrix, which is required for the invasion of tumor cells into the surrounding normal tissue, and MMP expression has been found to correlate positively with glioma invasiveness (24). The gelatinases MMP-2 and MMP-9 in glioblastoma have received particular attention, and it has been shown that human glioblastomas produce more MMP-2 than lower-grade gliomas, and that this expression correlates with their invasiveness (25-30). We therefore did gelatin zymography to determine whether OLIG2 expression in U12-1 cells affects the release of MMP-2 and MMP-9 into the culture medium. The OLIG2-expressing cells produced markedly lower MMP-2 levels than the Tet-on cells, but MMP-9 was not detected in the culture supernatants of either cell type (Supplementary Fig. S1). Neural stem cells of the human embryonic central nervous system, which undergo extensive migration within the brain, have also been shown to express MMP-2 but not MMP-9 (31), which suggests that MMP-2 expression is related to the invasiveness of cells in the human central nervous system. Together, these observations suggest that the inhibitory effect of OLIG2 expression on U12-1 cell invasion might be attributable, at least in part, to the down-regulation of MMP-2 production.

OLIG2 Activates RhoA in U12-1 Cells

The Rho family of GTPases (Rho, Rac, and Cdc42) regulates the migration of various cell types, including glioma cells (32). To examine whether OLIG2 expression affects the activity of these GTPases, we determined the amounts of the GTP-bound forms of RhoA, Rac1, and Cdc42 in the Tet-on and Tet-off cells. To do so, we purified glutathione S-transferase (GST) fusion proteins containing the Rho-binding domain of Rhotekin (GST-Rhotekin-RBD) or the Cdc42- or Rac-interactive binding motif of PAK2 (GST-PAK2-CRIB). These proteins were then used in "pull-down" assays. OLIG2 expression increased the amount of GTP-bound RhoA by ~6-fold (Fig. 2, *left*). In contrast, Rac1 activity was not affected (Fig. 2, *middle*) and that of Cdc42 was reduced by OLIG2 expression (Fig. 2, *right*). We therefore subsequently focused on OLIG2-induced RhoA activation.

OLIG2 Expression in U12-1 Cells Induces the Formation of Stress Fibers and Focal Adhesions

Rho signaling regulates the rearrangement of the actin cytoskeleton and the formation of focal adhesion complexes (33). Given that RhoA is activated by OLIG2 expression in U12-1 cells, we next assessed whether OLIG2 affects the formation of actin stress fibers and the localization of paxillin (a major constituent of focal adhesions) by confocal microscopy. Tet-on (OLIG2^{−}) cells exhibited polarity with an elongated cell body and membrane protrusions containing filamentous-actin at their leading edge but lacked large focal adhesions (Fig. 3A and B). These characteristics suggested that the cells possessed the ability to migrate in a directed manner. In contrast, almost all Tet-off (OLIG2^{+}) cells had a dense

meshwork of filamentous-actin with discrete localizations of paxillin at the termini of actin bundles, which is indicative of focal adhesions (Fig. 3A and C). In addition, the number of cells exhibiting polarity was significantly reduced by OLIG2 expression (Fig. 3D). In general, hyperactivation of RhoA also results in the formation of extensive stress fiber networks and large, stable, peripherally located focal adhesion complexes as well as eliminating both cell polarity and membrane protrusions (34-39), which is consistent with the phenotype of the OLIG2-expressing U12-1 cells. These results suggest that OLIG2 induces the formation of stress fibers and focal adhesions as well as eliminating cell polarity and membrane protrusions.

OLIG2-Mediated Up-Regulation of $p27^{Kip1}$ Does Not Affect RhoA Activation but Helps Inhibit U12-1 Cell Migration

Cytoplasmic $p27^{Kip1}$ was recently shown to regulate cell migration independently of its role as an inhibitor of cyclin-dependent kinases, as it was found to regulate actin dynamics in mouse embryonic fibroblasts by inhibiting RhoA activation, thereby promoting cell migration (40). In these cells, $p27^{Kip1}$ was shown to bind to RhoA and thereby inhibit its interaction with guanine nucleotide exchange factors (GEF). Given that OLIG2 increases the expression of $p27^{Kip1}$ in U12-1 cells (14), we investigated the possibility that OLIG2 increases RhoA activity by regulating cytoplasmic $p27^{Kip1}$. Consistent with previous observations, mouse embryonic fibroblasts lacking $p27^{Kip1}$ showed impaired migration (Supplementary Fig. S2A) and elevated Rho-GTP levels (Supplementary Fig. S2B). In contrast, depletion of $p27^{Kip1}$ by RNA interference promoted OLIG2-expressing U12-1 cell motility (Fig. 4A) but did not significantly affect OLIG2-induced RhoA activation (Fig. 4B). These data suggest that increased $p27^{Kip1}$ expression is not essential for RhoA activation; instead, it helps suppress the motility of OLIG2-expressing U12-1 cells.

OLIG2 Decreases the Expression Level of RhoGAP8 mRNA in U12-1 Cells

All regulatory GTPases, including RhoA, exist in inactive, GDP-bound and active, GTP-bound conformations. The
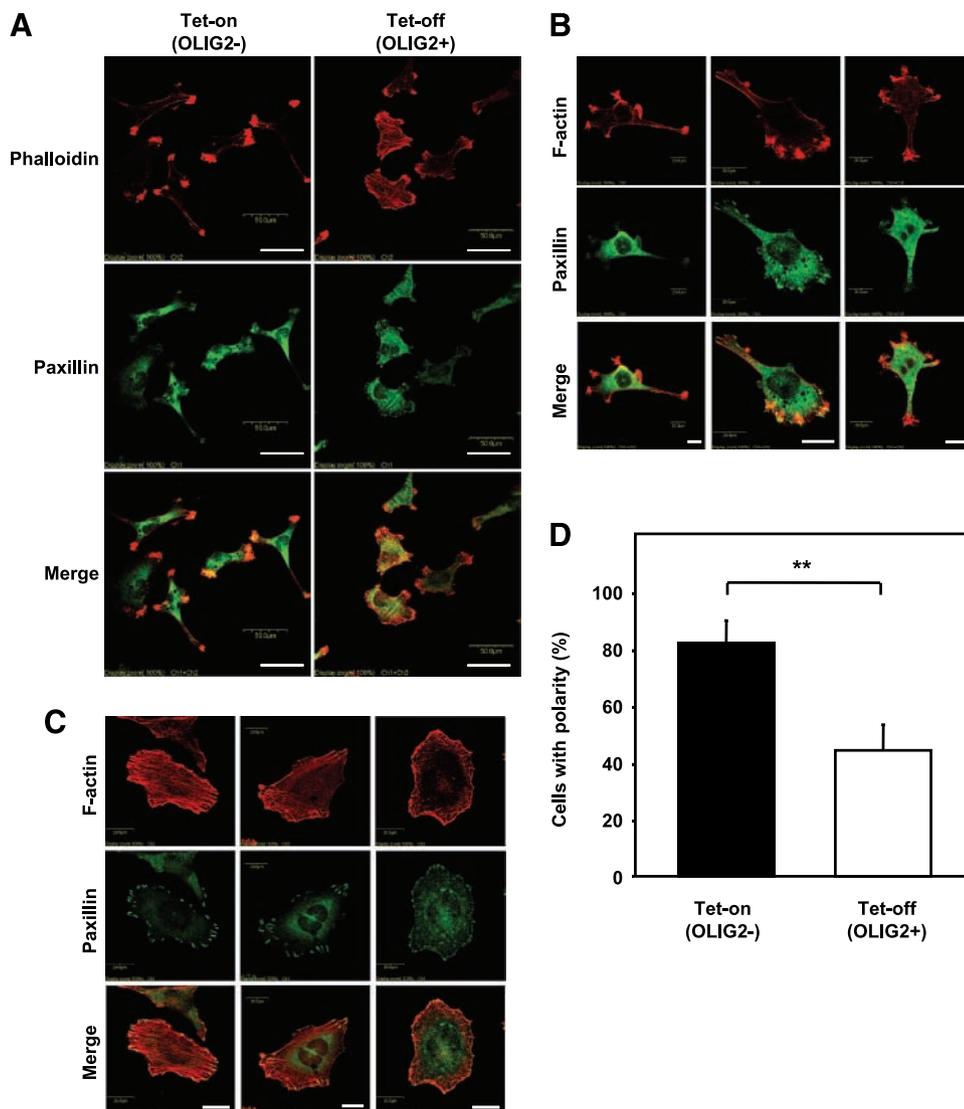
FIGURE 3. OLIG2 expression in U12-1 cells induces stress fiber formation, focal adhesion assembly, and disruption of cell polarity. Cells were grown in Tet-on or Tet-off medium for 48 h, transferred to glass chamber slides, and cultured for an additional 24 h. They were then fixed, permeabilized, stained with rhodamine-phalloidin to visualize filamentous-actin (*red*) and with anti-paxillin antibodies to visualize focal adhesions (*green*), and examined by confocal microscopy. **A.** Representative micrographs from three independent experiments. Scale bars, 50 μm. **B** and **C.** Higher-magnification images of the Tet-on and Tet-off cells, respectively. Scale bars, 20 μm. **D.** The proportion of cells with polarity among the total number of cells observed. Polarity was defined by polarity index, which was calculated as the maximum cell length/maximum cell width ratio, and the number of cells with polarity index ≥ 3 was counted after examination with a confocal laser-scanning microscope. Absolute numbers of cells with polarity are 78 of 95 Tet-on cells and 43 of 97 Tet-off cells. Columns, means from three independent experiments; bars, SD. **, $P < 0.01$ (Student's t test).

A

Time after a linear scratch

0   16   24   (hrs)

Tet-off
+
Control siRNA

Tet-off
+
p27 siRNA

FIGURE 4. Investigation of the mechanism of RhoA activation by OLIG2. **A.** Effect of knockdown p27^{Kip1} expression on OLIG2-mediated motility inhibition. Cells were cultured in Tet-off medium for 24 h and transfected with p27^{Kip1} or control short interfering RNA for 48 h. The p27^{Kip1} short interfering RNA sequence has been described previously (14). The cells were wounded and incubated for an additional 24 h. Top, representative micrographs at the indicated times after wounding. Scale bars, 200 μm. Bottom, quantitative data from three independent experiments; columns, means; bars, SD. *, $P < 0.05$; **, $P < 0.01$ (Student's t test). **B.** Effect of knockdown p27^{Kip1} expression on OLIG2-mediated RhoA activation. The active form of RhoA was precipitated from cell lysates and subjected to immunoblot analysis with anti-Rho antibodies. Cell lysates were also subjected directly to immunoblot analysis with the same antibodies as well as with anti-OLIG2 antibodies. **C.** Expression of RhoGEFs and RhoGAPs in the absence or presence of OLIG2. Cells were grown in Tet-on or Tet-off medium for 72 h, after which total RNA were extracted and semiquantitative reverse transcription-PCR analysis for two RhoGEFs (p115RhoGEF and LARG) and two RhoGAPs (p190RhoGAP and RhoGAP8) using specific primers was done as described in Materials and Methods.

■ Tet-off + Control siRNA
▨ Tet-off + p27siRNA

C

Tet: ON   OFF

p115RhoGEF
LARG
p190RhoGAP
RhoGAP8
OLIG2
GAPDH

B p27 siRNA: −   −   +   +

Tet: on   off   on   off

Active RhoA
Total RhoA
OLIG2
p27
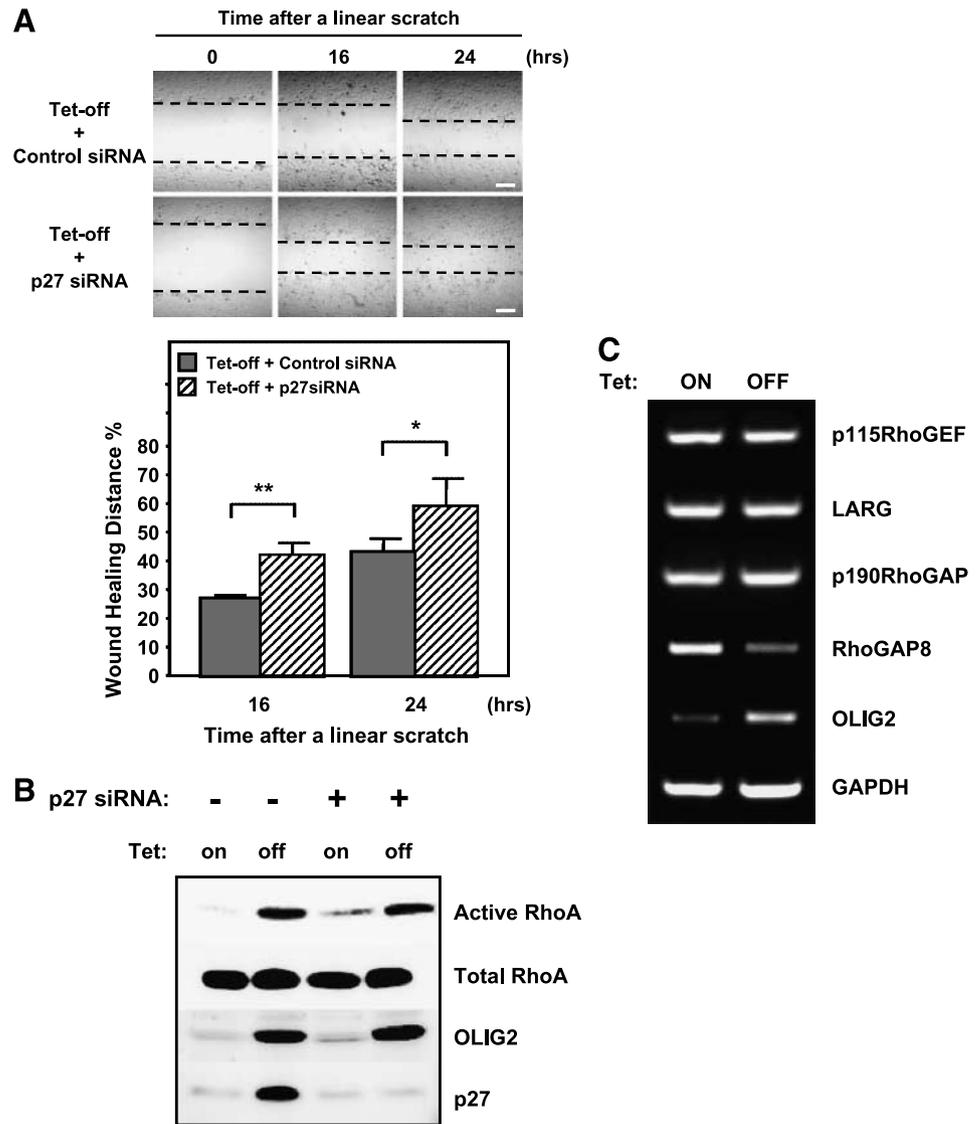
interconversion between these two forms is strictly regulated by a large family of GEFs that promote the release of bound GDP and facilitate GTP binding (41), and by a similarly large family of GTPase-activating proteins that stimulates the intrinsic GTPase activity of Rho family GTPases to promote their return to the inactive state (42). To investigate the possibility that OLIG2 increases RhoA activity by transcriptionally regulating the expression of RhoGEFs and/or RhoGAPs, we examined the transcriptomes of U12-1 cells that had been cultured in Tet-on or Tet-off medium by cDNA microarray analysis (Table 1) and confirmed the altered expression in four genes (*p115RhoGEF, LARG, p190RhoGAP*, and *RhoGAP8*) listed in Table 1 by semiquantitative reverse transcription-PCR analysis (Fig. 4C). We failed to observe differences in the expression levels of p115RhoGEF, LARG, and p190RhoGAP mRNA, but the level of RhoGAP8 mRNA was markedly decreased by OLIG2 expression. Thus, the inhibitory effect of OLIG2 on cell migration might be mediated by the decreased expression of RhoGAP8.

Expression of C3 Transferase Attenuates the OLIG2-Induced Inhibition of Cell Migration

To confirm that the activation of RhoA is causally related to the inhibitory effect of OLIG2 on cell motility, we transfected U12-1 cells with a bicistronic plasmid that expresses Flag-tagged C3 transferase and enhanced green fluorescent protein (EGFP). C3 is a *Clostridium botulinum* ADP-ribosyl transferase that inhibits the activation of all three mammalian Rho isoforms (RhoA, -B, and -C) by catalyzing their ADP-ribosylation (43). Consistent with previous observations with other cell types (44, 45), transfection of U12-1 cells with the C3 plasmid resulted in the ADP-ribosylation of RhoA. This effect was apparent from the decreased levels of GTP-bound RhoA and the decreased total RhoA mobility on SDS-polyacrylamide gels (Fig. 5A). The expression of C3 also eliminated the stress fibers and focal adhesions from Tet-off cells (Fig. 5B) as well as significantly attenuating the inhibitory effect of OLIG2 on U12-1 cell migration in the wound closure assay (Fig. 5C and D). In addition, it induced cell elongation at the wound edge (Fig. 5E);

Table 1. Microarray Analysis of Various Rho-Related Genes in U12-1 Cells in the Absence (Tet-on) or Presence (Tet-off) of OLIG2

Gene name (human)	GenBank accession no.	Cy5 Intensity (Tet-on)	Cy3 Intensity (Tet-off)	Cy3/Cy5 ratio
p115RhoGEF	BC014994	810	742	0.92
RhoGEF10	NM_014629	381	395	1.04
LARG	AF180681	193	115	0.60
Rho/Rac GEF18	BC005155	455	469	1.03
RhoE	S82240	557	495	0.89
p190RhoGAP	U17032	972	831	0.86
RhoGAP8	AF195968	86	47	0.56
RhoGDI α	BC009759	324	136	0.42
RhoGDI β	BC009200	88	63	0.72
RhoB	X06820	792	960	1.21
p160ROCK (ROCK1)	U43195	1,093	1,509	1.38
Rho kinase (ROCK2)	D87931	322	234	0.73
LIM kinase1	U62293	351	466	1.33
LIM kinase2	D45906	156	143	0.92
Vinculin	M33308	63	36	0.58
α-Actinin	X55187	1,087	1,188	1.09
Profilin1	BC006768	7,185	6,681	0.93

in these cells, the expression of C3 was confirmed by the bicistronic expression of EGFP (Fig. 5F). These data suggest that RhoA activation is essential for OLIG2-mediated inhibition of U12-1 cell migration.

OLIG2 Expression Results in RhoA Activation Around the Whole Perimeter of U12-1 Cells

Rho family GTPases function as molecular switches in signal transduction, and their ability to regulate cell behavior, such as migration, suggests the existence of a temporal and spatial control of their activity that might not be evident in biochemical assays (46). We therefore investigated the effect of OLIG2 on the subcellular localization and spatiotemporal regulation of RhoA in individual live cells by using FRET with the Raichu-RhoA probe (47). Thus, U12-1 cells expressing Raichu-RhoA were excited at 440 nm and imaged for cyan (CFP) and yellow (YFP) fluorescent proteins at 480 and 535 nm, respectively. The YFP/CFP fluorescence intensity ratio served as a measure of the FRET efficiency of the probe, which reflects its GTP/GDP ratio. RhoA has been shown to regulate membrane protrusion as well as cell body contractility in wounded monolayer cells and randomly migrating cells (48). Consistent with these observations, we observed RhoA activation during extending membrane protrusions and retracting tails of U12-1 Tet-on cells, with only minimal RhoA activity being detectable in the cell body (Fig. 6; Supplementary Movie S1A and B). In contrast, the high activity of RhoA was sustained around almost the entire periphery of U12-1 Tet-off cells, which exhibited few protrusions (Fig. 6; Supplementary Movie S2A and B). These results suggest that OLIG2 alters the cell morphology and inhibits cell ability via the hyperactivation of RhoA throughout the whole perimeter of the cell, which might be due to decreased turnover of RhoA in U12-1 cells.

Discussion

OLIG2 expression levels vary among gliomas (7-9) and the biological function of this transcription factor in these tumors was unclear. However, we have previously shown that OLIG2 inhibits glioma cell proliferation by inducing p27^{Kip1} expression (14). Furthermore, we have shown here that OLIG2 inhibits the motility of glioma cells by activating RhoA, a member of the Rho family of GTPases.
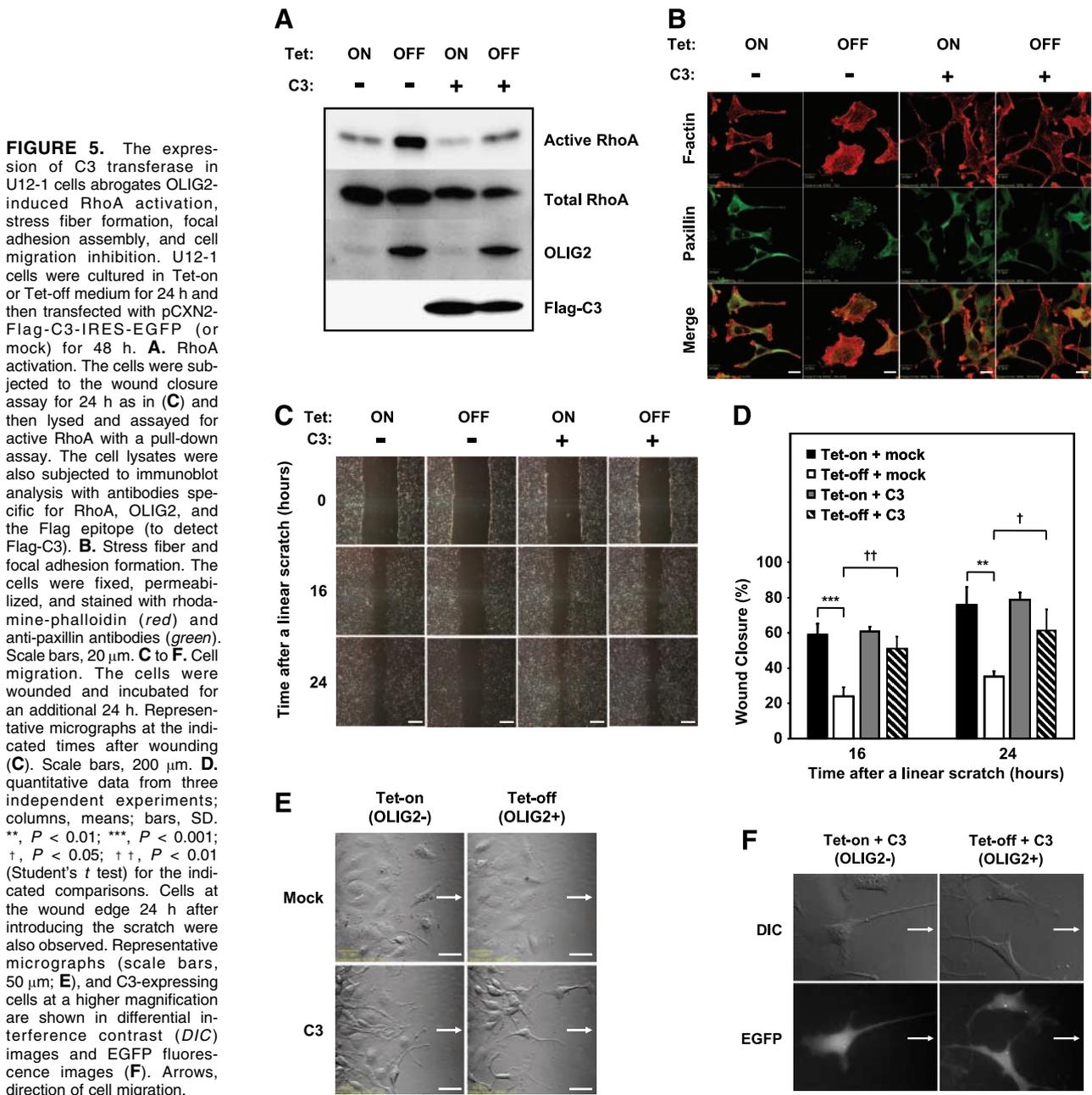
RhoA regulates cell body contraction in migrating cells by activating its downstream targets Rho-associated kinase (ROCK) and mDia and thereby promoting the assembly of actomyosin (23, 49). ROCK increases the phosphorylated myosin light chain levels, both by inhibiting myosin light chain phosphatase and by directly phosphorylating myosin light chain (50, 51). mDia interacts with IRSp53 (52), which promotes the actin polymerization mediated by the actin-related protein 2/3 complex (53). However, the mechanisms which regulate RhoA activity during cell migration are not well characterized. Similarly, the functions of ROCK and mDia are also not fully understood.
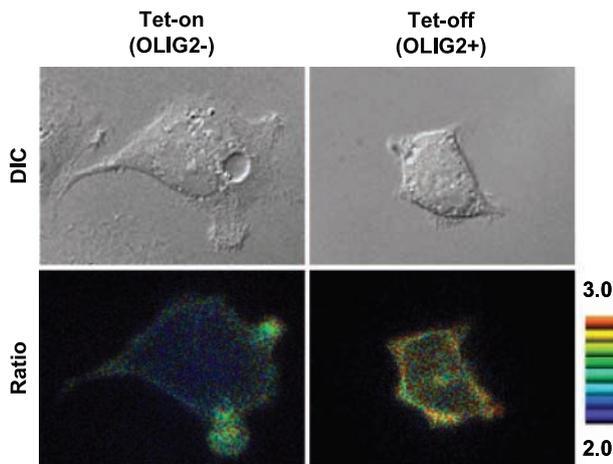
Some human cancers show increased Rho expression. Cancer-associated mutations in Rho regulators have also been characterized (54). Thus, Rho signaling pathways may be a potential target for cancer therapy. Indeed, ROCK inhibitors, including Wf-536 and Y27632, inhibit the metastatic growth of mammalian tumor cells (55, 56). However, in human gliomas, the expression levels of RhoA and RhoB have been found to be inversely correlated with tumor grade, being lowest in glioblastomas (57). Furthermore, inhibition of ROCK increases the motility of glioblastoma cell lines, including U251MG and U87MG, an effect that is accompanied by increased numbers of cell processes and membrane ruffling and the collapse of actin stress fibers (58). Moreover, overexpression of RhoA in U87MG cells up-regulates both MT1-MMP expression and CD44 shedding from the cell surface, thereby decreasing cell migration on hyaluronic acid (59). Consistent with these observations, we showed here that C3-mediated inactivation of Rho attenuates the OLIG2-mediated inhibition of U12-1 cell migration. The apparent difference in the effects of Rho on cell motility between gliomas and other tumor cell types suggests that the role of Rho in cell migration is dependent on cell type. Supporting this idea, RhoA facilitates phagocytic activity and cell migration in Swiss 3T3 cells (60), whereas overexpression of active RhoA inhibits motility in Madin-Darby canine kidney cells (61). It is possible that such differences are

attributable to differences in the basal level of activated RhoA. The speed of cell migration is determined by a biphasic response to adhesion strength, with fast migration occurring at intermediate adhesion strength, and slow migration occurring at low or high adhesion strength. Cell migration speed thus depends on a balance between adhesion and contraction, which are in turn dependent on focal adhesions and actomyosin dynamics, respectively (62, 63). Given that Rho family proteins regulate both the formation of focal adhesions and actomyosin dynamics, it is possible that an optimal level of RhoA activity may be needed for rapid migration; deviations from this optimal level may thus reduce migration speed. Indeed, membrane protrusions were apparent in U12-1 Tet-on cells, which exhibit

an intermediate level of RhoA activity (Fig. 6; Supplementary Movie S1A and B), but the formation of such protrusions was attenuated in Tet-off cells, in which the activity of RhoA is increased by OLIG2 (Fig. 6; Supplementary Movie S2A and B).

We also showed here that OLIG2 expression down-regulates the activity of Cdc42 (Fig. 2, *right*), a key regulator of cell polarity. Consistent with this observation, U12-1 cell polarization was inhibited by OLIG2 expression (Fig. 3D). The role of Cdc42 in glioma cell migration is unknown. However, the expression of a dominant negative form of Cdc42 (N17Cdc42) greatly reduced the polarization of migrating astrocytes, whereas dominant negative forms of Rac (N17Rac) or Rho

FIGURE 5. The expression of C3 transferase in U12-1 cells abrogates OLIG2-induced RhoA activation, stress fiber formation, focal adhesion assembly, and cell migration inhibition. U12-1 cells were cultured in Tet-on or Tet-off medium for 24 h and then transfected with pCXN2-Flag-C3-IRES-EGFP (or mock) for 48 h. **A.** RhoA activation. The cells were subjected to the wound closure assay for 24 h as in (**C**) and then lysed and assayed for active RhoA with a pull-down assay. The cell lysates were also subjected to immunoblot analysis with antibodies specific for RhoA, OLIG2, and the Flag epitope (to detect Flag-C3). **B.** Stress fiber and focal adhesion formation. The cells were fixed, permeabilized, and stained with rhodamine-phalloidin (*red*) and anti-paxillin antibodies (*green*). Scale bars, 20 μm. **C** to **F.** Cell migration. The cells were wounded and incubated for an additional 24 h. Representative micrographs at the indicated times after wounding (**C**). Scale bars, 200 μm. **D.** quantitative data from three independent experiments; columns, means; bars, SD. **, $P < 0.01$; ***, $P < 0.001$; †, $P < 0.05$; ††, $P < 0.01$ (Student's t test) for the indicated comparisons. Cells at the wound edge 24 h after introducing the scratch were also observed. Representative micrographs (scale bars, 50 μm; **E**), and C3-expressing cells at a higher magnification are shown in differential interference contrast (*DIC*) images and EGFP fluorescence images (**F**). Arrows, direction of cell migration.

FIGURE 6. FRET imaging of active RhoA in the absence or presence of OLIG2. U12-1 cells were plated on glass-bottomed dishes in Tet-on or Tet-off medium and transfected with a plasmid for the Raichu-RhoA probe. Differential interference contrast (*DIC*) as well as CFP and YFP fluorescence images were recorded every 4 min for 12 h with a time-lapse epifluorescence microscope. Ratio images of YFP/CFP represent FRET efficiency. Representative differential interference contrast images (*top*) and pseudocolor ratio images (*bottom*; scale on *right*). The corresponding video files are provided as Supplementary Movies S1A and B and S2A and B.

(N19Rho) had no effect (64). Our observations suggest that the OLIG2-induced reduction in Cdc42 activity, in addition to the increase in RhoA activity, might help inhibit glioma cell migration.

Although the mechanism by which OLIG2 increased RhoA activity in gliomas remains to be cleared in this study, we found that the expression of RhoGAP8 was decreased by OLIG2. It has been reported that RhoGAP8 interacts with cortactin to enhance migration in 293T cells (65, 66), which is consistent with our observation in U12-1 cells. Thus, the inhibitory effect of OLIG2 on cell migration might be mediated by affecting the expression levels of genes such as *RhoGAP8*, which contribute directly to RhoA activation. Guanine nucleotide dissociation inhibitors (GDI) constitute another group of Rho family GTPase regulators; GDIs thus maintain the GTPases in the cytoplasm in their GDP-bound form. Notably, our microarray analysis revealed that OLIG2 induction decreased the expression level of *Rho-GDI* genes in U12-1 cells, but immunoblot analysis showed that the abundance of the encoded proteins was not affected (Supplementary Fig. S3).

Finally, OLIG2 plays an important role in the differentiation of oligodendrocytes (1-4) by negatively regulating the default pathway of astrocytic differentiation (67-70). In addition, the stellation of astrocytes requires the inactivation of RhoA (71-74). OLIG2 may therefore negatively regulate not only the astrocytic fate of glial progenitors but also the adoption of astrocyte morphology during development.

Materials and Methods
Cell Culture and Transfection

The glioblastoma cell line U12-1 has been described previously (14). The cells were maintained under an atmosphere of 5% CO_2 at 37°C in Tet-on medium, which consists of DMEM supplemented with 10% fetal bovine serum, 2 mmol/L of L-glutamine, penicillin-streptomycin, G418, hygromycin B, and the tetracycline analogue doxycycline (50 ng/mL). OLIG2 expression was induced by transferring the cells to Tet-off medium, which is the same as Tet-on medium except for the lack of doxycycline. The Fugene HD reagent (Roche) was used to transfect cells with pCXN2-Flag-C3-IRES-EGFP (kindly provided by N. Mochizuki), which contains the coding sequences for Flag epitope–tagged C3 transferase and EGFP upstream and downstream, respectively, of an internal ribosomal entry site (IRES). Cells were transfected with the Raichu-RhoA plasmid by using LipofectAMINE 2000 (Invitrogen).

Wound Closure Assay

The wound closure assay was done as described (75). U12-1 cells were grown in Tet-on or Tet-off medium for 48 h. The confluent cells were then incubated in the corresponding medium containing 0.05% serum for 24 h, wounded by scratching the monolayer with a pipette tip, washed twice with PBS, allowed to migrate in DMEM containing 10% fetal bovine serum for the indicated times, and photographed. The assay was done in triplicate. To eliminate the possible influence of cell proliferation, cells were treated with mitomycin C (10 μg/mL; Sigma) for 3 h before scratching; we confirmed that this treatment blocked proliferation by determining growth curves (data not shown). To examine the effect of C3 on cell migration, cells were incubated in Tet-on or Tet-off medium for 24 h and then transfected with the C3 expression vector for 48 h before wounding. The cells were subsequently lysed in a solution containing 10 mmol/L of Tris-HCl (pH 7.5), 150 mmol/L of NaCl, 1% Triton X-100, 10% glycerol, 5 mmol/L of EDTA, 1 mmol/L of phenylmethylsulfonyl fluoride, and protease inhibitor mixture (Complete, Roche), and the cell lysates were subjected to immunoblot analysis with antibodies specific for the Flag epitope (Sigma) to confirm the expression of C3.

Matrigel Invasion Assay

Cell invasion assays were done with Matrigel-coated membrane filter inserts that have a pore size of 8 μm (BD Bioscience). U12-1 cells were first cultured for 48 h in Tet-on or Tet-off medium and then for 24 h in the corresponding medium containing 0.05% serum. The cells (5×10^4) were then suspended in 200 μL of DMEM supplemented with 0.5% serum and 0.1% bovine serum albumin (with or without doxycycline) and transferred to the upper surface of each insert. After incubation for 16 h using a 10% serum stimulus in the lower chamber, the remaining cells were removed from the upper side of the membrane by wiping, and the cells that had passed through to the lower side of the insert were fixed with 100% methanol and stained with 0.04% crystal violet. The number of cells that had invaded was then quantified by counting those in five random fields (20×) of each membrane. Experiments were done in triplicate.

Assay of GTPase Activity

The GTPase activities of RhoA, Rac1, and Cdc42 were determined as described previously (76). In brief, GST-Rhotekin-RBD and GST-PAK2-CRIB fusion proteins were

produced in *Escherichia coli* BL21 cells. To measure RhoA activity, U12-1 cells cultured for 72 h in Tet-on or Tet-off medium were lysed in a solution containing 50 mmol/L of Tris-HCl (pH 7.5), 100 mmol/L of NaCl, 1% Nonidet P40, 10% glycerol, 1 mmol/L of EDTA, 5 mmol/L of $MgCl_2$, 50 mmol/L of NaF, 1 mmol/L of sodium orthovanadate, 1 mmol/L of DTT, 1 mmol/L of phenylmethylsulfonyl fluoride, and protease inhibitor mixture (Complete). The cell lysates were centrifuged at $5,000 \times g$ for 5 min at 4°C, and the resulting supernatants (2 mg of protein) were incubated for 1 h at 4°C (with rotation) with 15 μg of GST-Rhotekin-RBD bound to glutathione-Sepharose 4B beads (Amersham Pharmacia Biotech). The beads were collected by centrifugation ($20,000 \times g$, 30 s, 4°C) and washed thrice. The bound proteins were eluted with SDS sample buffer and subjected to immunoblot analysis with rabbit polyclonal antibodies specific for RhoA (1:500 dilution; Santa Cruz Biotechnology) and horseradish peroxidase–conjugated secondary antibodies (1:2,000; Biosource). Immune complexes were visualized with enhanced chemiluminescence reagents (Amersham Pharmacia Biotech) and quantified with a LAS1000 image analyzer (Fuji Film). To measure Rac1 or Cdc42 activity, U12-1 cells were lysed in a solution containing 25 mmol/L of HEPES-NaOH (pH 7.5), 150 mmol/L of NaCl, 1% Nonidet P40, 10% glycerol, 1 mmol/L of EDTA, 10 mmol/L of $MgCl_2$, 1 mmol/L of phenylmethylsulfonyl fluoride, and protease inhibitor mixture (Complete). The cell lysates were clarified by centrifugation ($13,000 \times g$, 1 min, 4°C), and the resulting supernatants (2 mg of protein) were incubated for 1 h at 4°C (with rotation) with 15 μg of GST-PAK2-CRIB bound to glutathione-Sepharose 4B beads. The bead-bound proteins were subjected to immunoblot analysis with rabbit polyclonal antibodies specific for Rac1 (1:500) or Cdc42 (1:200; Santa Cruz Biotechnology). Cell lysates were also subjected to immunoblot analysis with antibodies specific for the corresponding GTPase and OLIG2 (13).

Immunocytofluorescence and Confocal Microscopy

U12-1 cells grown on Lab-Tek chamber slides (Nalge Nunc) in Tet-on or Tet-off medium were fixed with 3% paraformaldehyde in PBS for 15 min, permeabilized with 0.5% Triton X-100 in PBS for 5 min, and incubated with 1% bovine serum albumin in PBS for 20 min at room temperature. They were then incubated overnight at 4°C with mouse monoclonal antibodies specific for paxillin (1:2,000; BD Transduction Laboratories), then for 1 h at room temperature with Alexa Fluor 488–conjugated secondary antibodies (Molecular Probes), and finally for 30 min at room temperature with Alexa Fluor 594–conjugated phalloidin (Molecular Probes). The cells were then examined with a confocal laser-scanning microscope equipped with a computer (MRC-1024; Bio-Rad Microscience). Using these images, the cells were categorized into two groups, polarized (polarity index ≥3) and nonpolarized (polarity index <3), in which polarity index was defined as the maximum cell length/maximum cell width ratio. The proportion of the cells with polarity among total cells was shown as a bar graph. cDNA microarray analysis experiments have been described previously (14).

Semiquantitative Reverse Transcription-PCR Analysis

Total RNA was isolated from U12-1 cells using TRI-Reagent (Sigma) according to the manufacturer's instructions and resuspended in RNA secure resuspension solution (Ambion Inc.). Reverse transcription was carried out with Superscript II RT (Invitrogen) according to the manufacturer's instruction. One hundred nanograms of the resulting first-strand cDNA was used as template and amplified by PCR using KOD-Plus DNA polymerase (Toyobo). Sequences of the oligonucleotide primer sets used for reverse transcription-PCR analysis are as follows: 5′-ACGAGCCTGCCAAGACCAAG-3′ (sense) and 5′-ATGA-CCTCCTGCCGCTTCAC-3′ (antisense) for p115RhoGEF, 5′-ACCGAACACCTGCCCAAAGA-3′ (sense) and 5′-TGA-GCCGGGCGAGATTTTAG-3′ (antisense) for LARG, 5′-TCCG-AGAAGAGGAGGGTGGA-3′ (sense) and 5′-AGCGGCCAT-GATCCAACTGT-3′ (antisense) for p190RhoGAP, 5′-GCCT-CCCACCAAGACACCAC-3′ (sense) and 5′-CCGAAGACA-CAGGCCAGGTT-3′ (antisense) for RhoGAP8, 5′-GCATG-CACGACCTCAACATC-3′ (sense) and 5′-CGCTCACC-AGTCGCTTCAT-3′ (antisense) for OLIG2, 5′-CTCATGACC-ACAGTCCATGC-3′ (sense) and 5′-TTACTCCTTGGAG-GCCATGT-3′ (antisense) for glyceraldehyde-3-phosphate dehydrogenase.

Visualization of RhoA Activity in Living Cells

FRET imaging of RhoA was done by using the Raichu-RhoA probe essentially as described previously (77). In brief, U12-1 cells were cultured in Tet-on or Tet-off medium for 48 h, plated on 3.5-cm glass-bottomed dishes (Asahi Techno Glass Co.), and transfected with the expression vector for Raichu-RhoA (kindly provided by M. Matsuda, Kyoto University, Japan). After 24 h, the cells were imaged every 4 min with an IX71 inverted microscope (Olympus) that was equipped with a cooled CCD camera (CoolSNAP HQ; Roper Scientific) and controlled by MetaMorph software (Molecular Device). For dual-emission ratio imaging, a 440AF21 excitation filter, a 455DRLP dichroic mirror, and two emission filters (480AF30 for CFP and 535AF26 for YFP; Omega Optical) were used. The cells were illuminated with a 75-W xenon lamp through a 12% ND filter (Olympus) and a 60× oil immersion objective lens. The exposure time was 0.5 s when the binning of the CCD camera was set to 4×4. After background subtraction, the YFP/CFP ratio image was generated with MetaMorph software. Imaging of each sample was repeated at least three times to confirm the reproducibility of the results.

Statistical Analysis

Data are presented as means ± SD and were compared by Student's *t* test. $P < 0.05$ was considered statistically significant.

References

1. Lu QR, Yuk D, Alberta JA, et al. Sonic hedgehog-regulated oligodendrocyte lineage genes encoding bHLH proteins in the mammalian central nervous system. Neuron 2000;25:317–29.

2. Takebayashi H, Yoshida S, Sugimori M, et al. Dynamic expression of basic helix-loop-helix Olig family members: implication of Olig2 in neuron and oligodendrocyte differentiation and identification of a new member, Olig3. Mech Dev 2000;99:143–8.

3. Zhou Q, Wang S, Anderson DJ. Identification of a novel family of oligodendrocyte lineage-specific basic helix-loop-helix transcription factors. Neuron 2000;25:331–43.

4. Zhou Q, Choi G, Anderson DJ. The bHLH transcription factor Olig2 promotes oligodendrocyte differentiation in collaboration with Nkx2.2. Neuron 2001;31:791–807.

5. Ligon KL, Fancy SP, Franklin RJ, Rowitch DH. Olig gene function in CNS development and disease. Glia 2006;54:1–10.

6. Ligon KL, Kesari S, Kitada M, et al. Development of NG2 neural progenitor cells requires Olig gene function. Proc Natl Acad Sci U S A 2006;103:7853–8.

7. Lu QR, Park JK, Noll E, et al. Oligodendrocyte lineage genes (OLIG) as molecular markers for human glial brain tumors. Proc Natl Acad Sci U S A 2001; 98:10851–6.

8. Marie Y, Sanson M, Mokhtari K, et al. OLIG2 as a specific marker of oligodendroglial tumour cells. Lancet 2001;358:298–300.

9. Yokoo H, Nobusawa S, Takebayashi H, et al. Anti-human Olig2 antibody as a useful immunohistochemical marker of normal oligodendrocytes and gliomas. Am J Pathol 2004;164:1717–25.

10. Aguirre-Cruz L, Mokhtari K, Hoang-Xuan K, et al. Analysis of the bHLH transcription factors Olig1 and Olig2 in brain tumors. J Neurooncol 2004;67:265–71.

11. Ligon KL, Alberta JA, Kho AT, et al. The oligodendroglial lineage marker OLIG2 is universally expressed in diffuse gliomas. J Neuropathol Exp Neurol 2004;63:499–509.

12. Mokhtari K, Paris S, Aguirre-Cruz L, et al. Olig2 expression, GFAP, p53 and 1p loss analysis contribute to glioma subclassification. Neuropathol Appl Neurobiol 2005;31:62–9.

13. Ohnishi A, Sawa H, Tsuda M, et al. Expression of the oligodendroglial lineage-associated markers Olig1 and Olig2 in different types of human gliomas. J Neuropathol Exp Neurol 2003;62:1052–9.

14. Tabu K, Ohnishi A, Sunden Y, et al. A novel function of OLIG2 to suppress human glial tumor cell growth via p27Kip1 transactivation. J Cell Sci 2006;119:1433–41.

15. Wennerberg K, Der CJ. Rho-family GTPases: it's not only Rac and Rho (and I like it). J Cell Sci 2004;117:1301–12.

16. Prendergast GC, Khosravi-Far R, Solski PA, Kurzawa H, Lebowitz PF, Der CJ. Critical role of Rho in cell transformation by oncogenic Ras. Oncogene 1995;10:2289–96.

17. Qiu RG, Chen J, McCormick F, Symons M. A role for Rho in Ras transformation. Proc Natl Acad Sci U S A 1995;92:11781–5.

18. Lin R, Bagrodia S, Cerione R, Manor D. A novel Cdc42Hs mutant induces cellular transformation. Curr Biol 1997;7:794–7.

19. Keely PJ, Westwick JK, Whitehead IP, Der CJ, Parise LV. Cdc42 and Rac1 induce integrin-mediated cell motility and invasiveness through PI(3)K. Nature 1997;390:632–6.

20. Chan AY, Coniglio SJ, Chuang YY, et al. Roles of the Rac1 and Rac3 GTPases in human tumor cell invasion. Oncogene 2005;24:7821–9.

21. Bouzahzah B, Albanese C, Ahmed F, et al. Rho family GTPases regulate mammary epithelium cell growth and metastasis through distinguishable pathways. Mol Med 2001;12:816–30.

22. Sahai E, Marshall CJ. RHO-GTPases and cancer. Nat Rev Cancer 2002;2:133–42.

23. Raftopoulou M, Hall A. Cell migration: Rho GTPases lead the way. Dev Biol 2004;265:23–32.

24. Nakada M, Okada Y, Yamashita J. The role of matrix metalloproteinases in glioma invasion. Front Biosci 2003;8:e261–9.

25. Kunishio K, Okada M, Matsumoto Y, Nagao S. Matrix metalloproteinase-2 and -9 expression in astrocytic tumors. Brain Tumor Pathol 2003;20:39–45.

26. Levicar N, Nuttall RK, Lah TT, Nutall RK. Proteases in brain tumour progression. Acta Neurochir (Wien) 2003;145:825–38.

27. Thorns V, Walter GF, Thorns C. Expression of MMP-2, MMP-7, MMP-9, MMP-10 and MMP-11 in human astrocytic and oligodendroglial gliomas. Anticancer Res 2003;23:937–44.

28. Wang M, Wang T, Liu S, Yoshida D, Teramoto A. The expression of matrix metalloproteinase-2 and -9 in human gliomas of different pathological grades. Brain Tumor Pathol 2003;20:65–72.

29. Komatsu K, Nakanishi Y, Nemoto N, Hori T, Sawada T, Kobayashi M. Expression and quantitative analysis of matrix metalloproteinase-2 and -9 in human gliomas. Brain Tumor Pathol 2004;21:105–12.

30. Guo P, Imanishi Y, Cackowski FC, et al. Up-regulation of angiopoietin-2, matrix metalloprotease-2, membrane type 1 metalloprotease, and laminin 5γ2 correlates with the invasiveness of human glioma. Am J Pathol 2005;166:877–90.

31. Frolichsthal-Schoeller P, Vescovi AL, Krekoski CA, Murphy G, Edwards DR, Forsyth P. Expression and modulation of matrix metalloproteinase-2 and tissue inhibitors of metalloproteinases in human embryonic CNS stem cells. Neuroreport 1999;10:345–51.

32. Ridley AJ. Rho GTPases and cell migration. J Cell Sci 2001;114:2713–22.

33. Narumiya S, Ishizaki T, Watanabe N. Rho effectors and reorganization of actin cytoskeleton. FEBS Lett 1997;410:68–72.

34. Ilic D, Furuta Y, Kanazawa S, et al. Reduced cell motility and enhanced focal adhesion contact formation in cells from FAK-deficient mice. Nature 1995;377:539–44.

35. Ren XD, Kiosses WB, Sieg DJ, Otey CA, Schlaepfer DD, Schwartz MA. Focal adhesion kinase suppresses Rho activity to promote focal adhesion turnover. J Cell Sci 2000;113:3673–8.

36. Arthur WT, Burridge K. RhoA inactivation by p190RhoGAP regulates cell spreading and migration by promoting membrane protrusion and polarity. Mol Biol Cell 2001;12:2711–20.

37. Cox EA, Sastry SK, Huttenlocher A. Integrin-mediated adhesion regulates cell polarity and membrane protrusion through the Rho family of GTPases. Mol Biol Cell 2001;12:265–77.

38. Sugimoto N, Takuwa N, Okamoto H, Sakurada S, Takuwa Y. Inhibitory and stimulatory regulation of Rac and cell motility by the G12/13-Rho and Gi pathways integrated downstream of a single G protein-coupled sphingosine-1-phosphate receptor isoform. Mol Cell Biol 2003;23:1534–45.

39. Vial E, Sahai E, Marshall CJ. ERK-MAPK signaling coordinately regulates activity of Rac1 and RhoA for tumor cell motility. Cancer Cell 2003;4:67–79.

40. Besson A, Gurian-West M, Schmidt A, Hall A, Roberts JM. p27Kip1 modulates cell migration through the regulation of RhoA activation. Genes Dev 2004;18:862–76.

41. Zheng Y. Dbl family guanine nucleotide exchange factors. Trends Biochem Sci 2001;26:724–32.

42. Moon SY, Zheng Y. Rho GTPase-activating proteins in cell regulation. Trends Cell Biol 2003;13:13–22.

43. Wilde C, Chhatwal GS, Schmalzing G, Aktories K, Just I. A novel C3-like ADP-ribosyltransferase from *Staphylococcus aureus* modifying RhoE and Rnd3. J Biol Chem 2001;276:9537–42.

44. Flatau G, Lemichez E, Gauthier M, et al. Toxin-induced activation of the G protein p21 Rho by deamidation of glutamine. Nature 1997;387:729–33.

45. Schmidt G, Sehr P, Wilm M, Selzer J, Mann M, Aktories K. Gln 63 of Rho is deamidated by *Escherichia coli* cytotoxic necrotizing factor-1. Nature 1997;387:725–9.

46. Pertz O, Hahn KM. Designing biosensors for Rho family proteins-deciphering the dynamics of Rho family GTPase activation in living cells. J Cell Sci 2004;117:1313–8.

47. Yoshizaki H, Ohba Y, Kurokawa K, et al. Activity of Rho-family GTPases during cell division as visualized with FRET-based probes. J Cell Biol 2003;162:223–32.

48. Pertz O, Hodgson L, Klemke RL, Hahn KM. Spatiotemporal dynamics of RhoA activity in migrating cells. Nature 2006;440:1069–72.

49. Mitchison TJ, Cramer LP. Actin-based cell motility and cell locomotion. Cell 1996;84:371–9.

50. Kaibuchi K, Kuroda S, Amano M. Regulation of the cytoskeleton and cell adhesion by the Rho family GTPases in mammalian cells. Annu Rev Biochem 1999;68:459–86.

51. Amano M, Fukata Y, Kaibuchi K. Regulation and functions of Rho-associated kinase. Exp Cell Res 2000;261:44–51.

52. Fujiwara T, Mammoto A, Kim Y, Takai Y. Rho small G-protein-dependent binding of mDia to an Src homology 3 domain-containing IRSp53/BAIAP2. Biochem Biophys Res Commun 2000;271:626–9.

53. Suetsugu S, Kurisu S, Oikawa T, Yamazaki D, Oda A, Takenawa T. Optimization of WAVE2 complex-induced actin polymerization by membrane-bound IRSp53, PIP(3), and Rac. J Cell Biol 2006;173:571–85.

54. Ridley AJ. Rho proteins and cancer. Breast Cancer Res Treat 2004;84:13–9.

55. Somlyo AV, Bradshaw D, Ramos S, Murphy C, Myers CE, Somlyo AP. Rho-kinase inhibitor retards migration and *in vivo* dissemination of human prostate cancer cells. Biochem Biophys Res Commun 2000;269:652–9.

56. Nakajima M, Hayashi K, Egi Y, et al. Effect of Wf-536, a novel ROCK inhibitor, against metastasis of B16 melanoma. Cancer Chemother Pharmacol 2003;52:319–24.

57. Forget MA, Desrosiers RR, Del M, et al. The expression of rho proteins decreases with human brain tumor progression: potential tumor markers. Clin Exp Metastasis 2002;19:9–15.

58. Salhia B, Rutten F, Nakada M, et al. Inhibition of Rho-kinase affects astrocytoma morphology, motility, and invasion through activation of Rac1. Cancer Res 2005;65:8792–800.

59. Annabi B, Bouzeghrane M, Moumdjian R, Moghrabi A, Béliveau R. Probing the infiltrating character of brain tumors: inhibition of RhoA/ROK-mediated CD44 cell surface shedding from glioma cells by the green tea catechin EGCg. J Neurochem 2005;94:906–16.

60. Takaishi K, Kikuchi A, Kuroda S, Kotani K, Sasaki T, Takai Y. Involvement of rho p21 and its inhibitory GDP/GTP exchange protein (rho GDI) in cell motility. Mol Cell Biol 1993;13:72–9.

61. Ridley AJ, Comoglio PM, Hall A. Regulation of scatter factor/hepatocyte growth factor responses by Ras, Rac, and Rho in MDCK cells. Mol Cell Biol 1995;15:1110–22.

62. DiMilla PA, Barbee K, Lauffenburger DA. Mathematical model for the effects of adhesion and mechanics on cell migration speed. Biophys J 1991;60:15–37.

63. Gupton SL, Waterman-Storer CM. Spatiotemporal feedback between actomyosin and focal-adhesion systems optimizes rapid cell migration. Cell 2006;125:1361–74.

64. Hall A. Rho GTPases and the control of cell behaviour. Biochem Soc Trans 2005;33:891–5.

65. Lua BL, Low BC. BPGAP1 interacts with cortactin and facilitates its translocation to cell periphery for enhanced cell migration. Mol Biol Cell 2004;15:2873–83.

66. Lua BL, Low BC. Filling the GAPs in cell dynamics control: BPGAP1 promotes cortactin translocation to the cell periphery for enhanced cell migration. Biochem Soc Trans 2004;32:1110–2.

67. Doetsch F. The glial identity of neural stem cells. Nat Neurosci 2003;6:1127–34.

68. Ross SE, Greenberg ME, Stiles CD. Basic helix-loop-helix factors in cortical development. Neuron 2003;39:13–25.

69. Fukuda S, Kondo T, Takebayashi H, Taga T. Negative regulatory effect of an oligodendrocytic bHLH factor OLIG2 on the astrocytic differentiation pathway. Cell Death Differ 2004;11:196–202.

70. Muroyama Y, Fujiwara Y, Orkin SH, Rowitch DH. Specification of astrocytes by bHLH protein SCL in a restricted region of the neural tube. Nature 2005;438:360–3.

71. Ramakers GJ, Moolenaar WH. Regulation of astrocyte morphology by RhoA and lysophosphatidic acid. Exp Cell Res 1998;245:252–62.

72. Kalman D, Gomperts SN, Hardy S, Kitamura M, Bishop JM. Ras family GTPases control growth of astrocyte processes. Mol Biol Cell 1999;10:1665–83.

73. Chen CJ, Liao SL, Huang YS, Chiang AN. RhoA inactivation is crucial to manganese-induced astrocyte stellation. Biochem Biophys Res Commun 2005;326:873–9.

74. Chen CJ, Ou YC, Lin SY, Liao SL, Huang YS, Chiang AN. L-Glutamate activates RhoA GTPase leading to suppression of astrocyte stellation. Eur J Neurosci 2006;23:1977–87.

75. Defilippi P, Truffa G, Stefanuto G, Altruda F, Silengo L, Tarone G. Tumor necrosis factor α and interferon γ modulate the expression of the vitronectin receptor (integrin β3) in human endothelial cells. J Biol Chem 1991;266:7638–45.

76. Tsuda M, Makino Y, Iwahara T, et al. Crk associates with ERM proteins and promotes cell motility toward hyaluronic acid. J Biol Chem 2004;279:46843–50.

77. Kurokawa K, Matsuda M. Localized RhoA activation as a requirement for the induction of membrane ruffling. Mol Biol Cell 2005;16:4294–303.

78. Nakayama K, Ishida N, Shirane M, et al. Mice lacking p27(Kip1) display increased body size, multiple organ hyperplasia, retinal dysplasia, and pituitary tumors. Cell 1996;85:707–20.

Oligodendrocyte Lineage Transcription Factor 2 Inhibits the Motility of a Human Glial Tumor Cell Line by Activating RhoA

Kouichi Tabu, Yusuke Ohba, Tadaki Suzuki, et al.

Updated version	Access the most recent version of this article at: http://mcr.aacrjournals.org/content/5/10/1099
Supplementary Material	Access the most recent supplemental material at: http://mcr.aacrjournals.org/content/suppl/2008/01/04/5.10.1099.DC1

Cited articles	This article cites 78 articles, 23 of which you can access for free at: http://mcr.aacrjournals.org/content/5/10/1099.full#ref-list-1
Citing articles	This article has been cited by 3 HighWire-hosted articles. Access the articles at: http://mcr.aacrjournals.org/content/5/10/1099.full#related-urls

E-mail alerts	Sign up to receive free email-alerts related to this article or journal.
Reprints and Subscriptions	To order reprints of this article or to subscribe to the journal, contact the AACR Publications Department at pubs@aacr.org.
Permissions	To request permission to re-use all or part of this article, use this link http://mcr.aacrjournals.org/content/5/10/1099. Click on "Request Permissions" which will take you to the Copyright Clearance Center's (CCC) Rightslink site.